# Spatiotemporal characterization of mercury isotope baselines and anthropogenic influences in lake sediment cores

**Ju Hyeon Lee[1], Sae Yun Kwon[1,2*], Runsheng Yin[3], Laura M. Motta[1], Aaron Y. Kurz[4], Seung-Il Nam[5]**

[1] Division of Environmental Science and Engineering, Pohang University of Science and Technology, 77 Cheongam-Ro, Nam Gu, Pohang 37673 South Korea

[2] Institute for Convergence Research and Education in Advanced Technology, Yonsei University, 85 Songdogwahak-Ro, Yeonsu-Gu, Incheon 21983 South Korea

[3] State Key Laboratory of Ore Deposit Geochemistry, Institute of Geochemistry, Chinese Academy of Sciences, 99 West Lincheng Road, Guiyang, Guizhou 550081 China

[4] Department of Earth and Environmental Sciences, University of Michigan, 1100 N. University Avenue, Ann Arbor, Michigan 48109 United States

[5] Division of Polar Paleoenvironment, Korea Polar Research Institute, 260 Songdomirae-ro, Yeonsu-gu, Incheon 21990 South Korea

* Corresponding author: Sae Yun Kwon (saeyunk@postech.ac.kr)

**Key Points:**

- Positive $\delta^{202}$Hg shifts together with mercury concentration in lake sediment cores from pre-industrial to present-day period are a widespread phenomenon.
- Magnitudes of $\delta^{202}$Hg and $\Delta^{199}$Hg changes are determined by the pre-industrial or baseline values in the sediment cores rather than the degree of mercury input.
- Sediment $\delta^{202}$Hg can be used as a proxy for monitoring changes in anthropogenic mercury sources for the Minamata Convention on Mercury.

This is the author manuscript accepted for publication and has undergone full peer review but has not been through the copyediting, typesetting, pagination and proofreading process, which may lead to differences between this version and the Version of Record. Please cite this article as doi: 10.1029/2020GB006904.

**Abstract**

Increasing mercury isotope ratios from pre-industrial (1510 – 1850) to present-day (1990 – 2014) in lake sediment cores have been suggested to be a global phenomenon. To assess factors leading to spatiotemporal changes, we compiled mercury concentration (THg) and mercury isotope ratios in twenty-two lake sediment cores located at various regions of the world. We find that the positive $\delta^{202}$Hg shifts together with THg increases from pre-industrial to present-day are a widespread phenomenon. This is caused by increased contribution of mercury from local to regional anthropogenic mercury emission sources, which have higher $\delta^{202}$Hg (-1.07±0.69‰, 1 s.d.) than pre-industrial sediments (-1.55±0.96‰, 1 s.d.). The positive $\Delta^{199}$Hg shifts were observed in fifteen lake sediment cores, which have low pre-industrial $\Delta^{199}$Hg (-0.20±0.32‰) compared to the sediment cores with near-zero to positive pre-industrial $\Delta^{199}$Hg (0.08±0.07‰). The magnitudes of $\delta^{202}$Hg ($r^2$ = 0.09) and $\Delta^{199}$Hg ($r^2$ = 0.20, both $p > 0.05$) changes from pre-industrial to present-day did not correlate with the magnitude of THg changes. Instead, the magnitudes of $\delta^{202}$Hg and $\Delta^{199}$Hg changes decreased with increasing pre-industrial $\delta^{202}$Hg and $\Delta^{199}$Hg values, suggesting that the baseline mercury isotope ratios play a more important role in determining the magnitude of mercury isotope changes compared to the degree of THg input. We suggest that the spatiotemporal assessments of $\delta^{202}$Hg in lake sediment cores can be used as an important proxy for monitoring changes in anthropogenic mercury sources for the Minamata Convention on Mercury.

## 1 Introduction

Mercury is a globally distributed atmospheric pollutant, which travels long distances in the form of gaseous elemental mercury ($Hg^0$). Gaseous $Hg^0$ is removed from the atmosphere via the foliar uptake (Demers et al., 2013; Zhou et al., 2021) or via oxidation to $Hg^{2+}$, which is readily deposited to the biosphere following sorption to particles ($Hg_P$) and/or precipitation (Selin, 2009). Since industrialization, anthropogenic activities alone have increased mercury emission by a factor of ~5 (Streets et al., 2017). Increased mercury loading to aquatic ecosystems can enhance microbial production of monomethylmercury (MeHg) (Benoit et al., 2003; Lindberg et al., 2007), which is a bioaccumulative toxin in food webs (Mergler et al., 2007). Humans are primarily exposed to MeHg via the consumption of fishery products (Sunderland, 2007).

In 2017, the Minamata Convention on Mercury (MC), a multilateral agreement to mitigate anthropogenic mercury emissions and human health from mercury pollution, has entered into force (UNEP, 2019). As a part of the MC, provisions have been established for a global monitoring program and a convention effectiveness evaluation (Article 19, 22) to understand spatiotemporal changes in mercury levels as well as its sources, processes, and fate in various environmental media. Since then, numerous studies have assessed temporal trends of mercury in diverse atmospheric samples ($Hg^0$, $Hg^{2+}$, $Hg_P$, precipitation) (Cheng et al., 2017; Dommergue et al., 2016) and biota (fish, bird eggs, polar bear) (Blukacz-Richards et al., 2017; Lee et al., 2016; McKinney et al., 2017) to gather insights on the changes in emissions, deposition, and ecosystem fate of mercury. Natural archives of sediment, peat, and ice cores have also been used to quantify long-term changes in the deposition of various atmospheric mercury species (Engstrom et al., 2014; Enrico et al., 2017; Zdanowicz et al., 2016; Zerkle et al., 2020). In particular, mercury in sediment

cores of lakes with large surface area relative to watershed area is thought to reflect delivery via precipitation and is less prone to diagenetic and hydrodynamic effects resulting in mobility and release compared to mercury in peat and marine sediment cores (Asmund & Nielsen, 2000; Cooke et al., 2020; Wasik et al., 2015). Recent studies reported consistent 3-5 fold enrichments in anthropogenic mercury relative to the pre-industrial period in lake sediment cores collected from various remote regions (Amos et al., 2015; Engstrom et al., 2014; Fitzgerald et al., 2005).

While mercury concentrations in lake sediment cores have been evaluated on a broad spatiotemporal scale, sources as well as atmospheric and biogeochemical processes leading to spatiotemporal trends in mercury isotope ratios are only beginning to be understood. Mercury isotopes undergo mass-dependent fractionation (MDF; $\delta^{202}$Hg) via various biotic and abiotic processes including methylation, demethylation, and mineral sorption (e.g., Blum et al., 2014; Kwon et al., 2020). Significant mass-independent fractionation of odd-mass number isotopes ($MIF_{odd}$; $\Delta^{199}$Hg, $\Delta^{201}$Hg) has been observed primarily during photo-reduction and photo-degradation of $Hg^{2+}$ and MeHg, respectively (Bergquist & Blum, 2007). Significant MIF of even-mass number isotopes ($MIF_{even}$; $\Delta^{200}$Hg, $\Delta^{204}$Hg) is thought to occur via photo-oxidation of $Hg^0$ in the atmosphere (Chen et al., 2012; Cai & Chen, 2016). Given the limited processes resulting in MIF, $\Delta^{199}$Hg has been used to interpret changes in mercury sources and/or processes in natural archives including sediment and ice cores (Guédron et al., 2016; Kurz et al., 2019; Yin et al., 2016a; Zerkle et al., 2020).

Recently, there has been a consensus from the literature that increasing $\Delta^{199}$Hg (by 0.1 to 0.3‰) in lake sediment cores from pre-industrial to present-day period is a global phenomenon

(Guédron et al., 2016; Kurz et al., 2019; Yin et al., 2016a). To explain this phenomenon, multiple hypotheses have been proposed. Kurz et al. (2019) proposed that the changes in global atmospheric chemical composition caused by increased levels of anthropogenic atmospheric pollutants can enhance $Hg^{2+}$ photo-reduction in precipitation and result in positive $\Delta^{199}Hg$ shifts in a remote Wyoming lake, U.S. In remote Tibetan lakes, decreased ice cover resulting in increased $Hg^{2+}$ photo-reduction in the water column was suggested as the main driver for the positive $\Delta^{199}Hg$ shifts (Yin et al., 2016a). In contrast, Guérdron et al. (2016) measured $\Delta^{199}Hg$ in a French lake surrounded by multiple mercury point sources and suggested that increased industrial mercury emissions, characterized by less negative $\Delta^{199}Hg$ compared to geogenic sources, is responsible for the $\Delta^{199}Hg$ changes. In addition, a recent study by Lepak et al. (2020b) observed positive temporal shifts in $\Delta^{199}Hg$ and $\delta^{202}Hg$ in nine lake sediment cores collected from remote regions of North America. The authors suggested that the magnitude of changes in mercury isotope ratios from pre-industrial to present-day period is governed by the amount of atmospheric mercury loading. As such, it is unclear whether the positive $\Delta^{199}Hg$ and $\delta^{202}Hg$ shifts are driven by site-specific or global changes in mercury sources or processes. The understanding of the linkages between the magnitude of mercury input and changes in mercury isotope ratios across a large spatiotemporal scale will also be important for using lake sediment cores as a proxy for global monitoring and effectiveness evaluation of the MC.

Here, we compiled mercury concentration and mercury isotope ratios of lake sediment cores from various locations of the world. Our aim was to 1) characterize spatiotemporal differences in mercury levels and isotope ratios, 2) gather insights into source- and/or process-driven changes in mercury isotope ratios, and 3) identify factors governing the magnitude of

changes in mercury isotope ratios relative to the changes in mercury input. We discuss our results in relation to the global monitoring and effectiveness evaluation objectives of the MC.

## 2 Materials and Methods

Total mercury (THg) concentration and mercury isotope ratios ($\delta^{202}$Hg, $\Delta^{199}$Hg, $\Delta^{200}$Hg) of twenty-two lake sediment cores were compiled from the literature (Cooke et al., 2013; Gray et al., 2013; Guédron et al., 2016; Kurz et al., 2019; Lepak et al., 2020a; Ma et al., 2013; Yin et al., 2016a, 2016b). For compilation, we first screened for sediment cores, which reported both THg and mercury isotope ratios prior to significant local anthropogenic mercury influences and/or those dating back to pre-industrialization. We then screened for sediment cores, which followed the standard mercury isotope ratio reporting and measurement system (Bergquist & Blum, 2009, Blum & Johnson, 2017) of using NIST SRM 3133 and NIST RM 8610 (also known as UM-Almadèn) as a bracketing and analytical standard, respectively, to ensure data quality. All lake sediment cores compiled in this study were dated by $^{210}$Pb using isotope-dilution, alpha spectrometry methods, and the constant rate of supply dating model (Table S1). The complete list of THg concentration and mercury isotope ratios associated with each sediment core and its depth and age dating are reported in our compiled data.

Based on the inventories of all-time anthropogenic mercury emissions from Streets et al. (2017), we set the pre-industrial period as years between 1510 and 1850. The present-day is set to years between 1990 and 2014, which is consistent with those referenced by Amos et al. (2015) and Li et al. (2020) using empirical assessments of mercury in various natural archives. Note that year 2014 is the earliest mercury isotope measurement available in our compiled data. To characterize

mercury levels and isotope baseline of the pre-industrial period, we calculate the average THg concentration and mercury isotope ratios spanning the years between 1510 and 1850 for each sediment core. For sediment cores without data prior to 1850 (five cores; Phantom, Cleaver, McLurg Lake in Manitoba, Canada, Lake Luitel in France, Lake Michigan in the U.S.) (Guédron et al., 2016; Ma et al., 2013; Yin et al., 2016b), we use the average THg concentration and mercury isotope ratios of three data points representing the deepest layer, which span years between 1873 and 1913. While these years represent the time during industrialization, the THg and mercury isotope ratios reflect those prior to significant local anthropogenic mercury emissions as suggested by the individual authors.

The spatiotemporal changes in mercury levels and isotope ratios are evaluated by 1) comparing the average THg concentration and mercury isotope ratios between the pre-industrial and present-day period, 2) by testing the significance of differences in THg concentration and mercury isotope ratios between the pre-industrial and present-day period, and 3) by assessing the significance of temporal trends in mercury isotope ratios for each sediment core. We calculate the average THg concentration and mercury isotope ratios reflecting years between 1990 and 2014 (present-day) for each sediment core. Several cores had only one data point spanning these years (three cores; El Junco, Laguna Negrilla in Peru, Perfect Lake in the Arctic). We did not take the average of the most recent three data points because they span years between 1964 and 1983, which are too old to include. We set the significant difference in the average mercury isotope ratios between the pre-industrial and present-day period as changes greater than the analytical uncertainty (2 standard deviation; 2SD) reported by individual studies compiled here; ±0.09‰ for $\delta^{202}$Hg, ±0.06‰ for $\Delta^{199}$Hg, and ±0.05‰ for $\Delta^{200}$Hg (Table S2). The Kruskal-Wallis test, which

assumes non-parametric data, was also used to test the significance of differences in THg and mercury isotope ratios between the pre-industrial and present-day periods. Based on the results of Shapiro-Wilk test for normality, the THg concentrations and mercury isotope ratios, except for the present-day unremote $\Delta^{200}$Hg, were not normally distributed (Table S3, Figure S1), which confirm the use of the Kruskal-Wallis test. The H-value is the test statistic for the Kruskal-Wallis test to calculate the p-value and the p-value (<0.05) indicates the significance of correlation between two variables. The two-tailed conventional linear trend test was used to verify the significance of temporal trends in THg and mercury isotope ratios over the pre-industrial to present-day period for each core. The slope indicates the direction of trend between two variables and the p-value (<0.05) indicates the significance of temporal trend (Table S4).

To characterize spatial differences in the changes in mercury levels and isotope ratios, the magnitude of differences in THg concentration and mercury isotope ratios between the pre-industrial and present-day periods are evaluated across different sampling locations of the lake sediment cores and between remote and unremote regions. The remote and unremote regions are categorized based on the proximity to local anthropogenic mercury emission sources and those characterized by the individual authors. Specifically, one sediment core from Lake Ballinger, Washington, U.S. (Gray et al., 2013) and three sediment cores from Manitoba, Canada (Phantom, Cleaver, McLurg Lake; Ma et al., 2013) are known to be impacted by local point mercury sources of lead, copper, and zinc smelters. One sediment core from Lake Luitel, Grenoble, France (Guérdron et al., 2016) and three sediment cores from Lake Michigan, U.S. (Yin et al., 2016b) have received diverse anthropogenic mercury sources of manufacturing industries and mining activities, originated from rapid industrialization since the mid-1850s. Five sediment cores

collected from the national forest in Wyoming, U.S. (Lost Lake; Kurz et al., 2019), the Peruvian Andes and Galápagos archipelago, Ecuador (El Junco, Laguna Negrilla; Cooke et al., 2013) and Tibetan Plateau, China (Qinghai, Nam Co; Yin et al., 2016a) are thought to be one of the most remote locations in the world. The remaining nine sediment cores are from the study by Lepak et al. (2020b), in which the authors described the lakes as generally remote and undisturbed from Alaska and Minnesota, U.S. and Newfoundland, Canada.

## 3 Results and Discussion

### 3.1 Spatiotemporal differences in mercury levels and isotope ratios

The locations of the sediment cores are skewed to the Northern Hemisphere and specifically North America (Figure 1). Elevated THg concentrations were observed in Laguna Negrilla, Peru (228-684 ng/g) (Cooke et al., 2013) and Phantom Lake, Manitoba, Canada (496-941 ng/g) (Ma et al., 2013) during the pre-industrial period (1510-1850) (Figure 1a), which were suggested to be impacted by mercury used during historical mining. Without these lake sediments (Laguna Negrilla, Phantom Lake), the THg concentrations were much lower (average; 99±57 ng/g, range; 17-249 ng/g, n = 142) and similar to those of pre-industrial sediments reported previously (~70 ng/g) (Fitzgerald et al., 2005; Engstrom et al., 2007, 2014). The present-day sediments had significantly higher and wide ranges in THg concentration (median; 265±2933 ng/g, range; 38-19076 ng/g, n = 103) compared to the pre-industrial sediments (Kruskal-Wallis test, $p < 0.05$, Table S5).

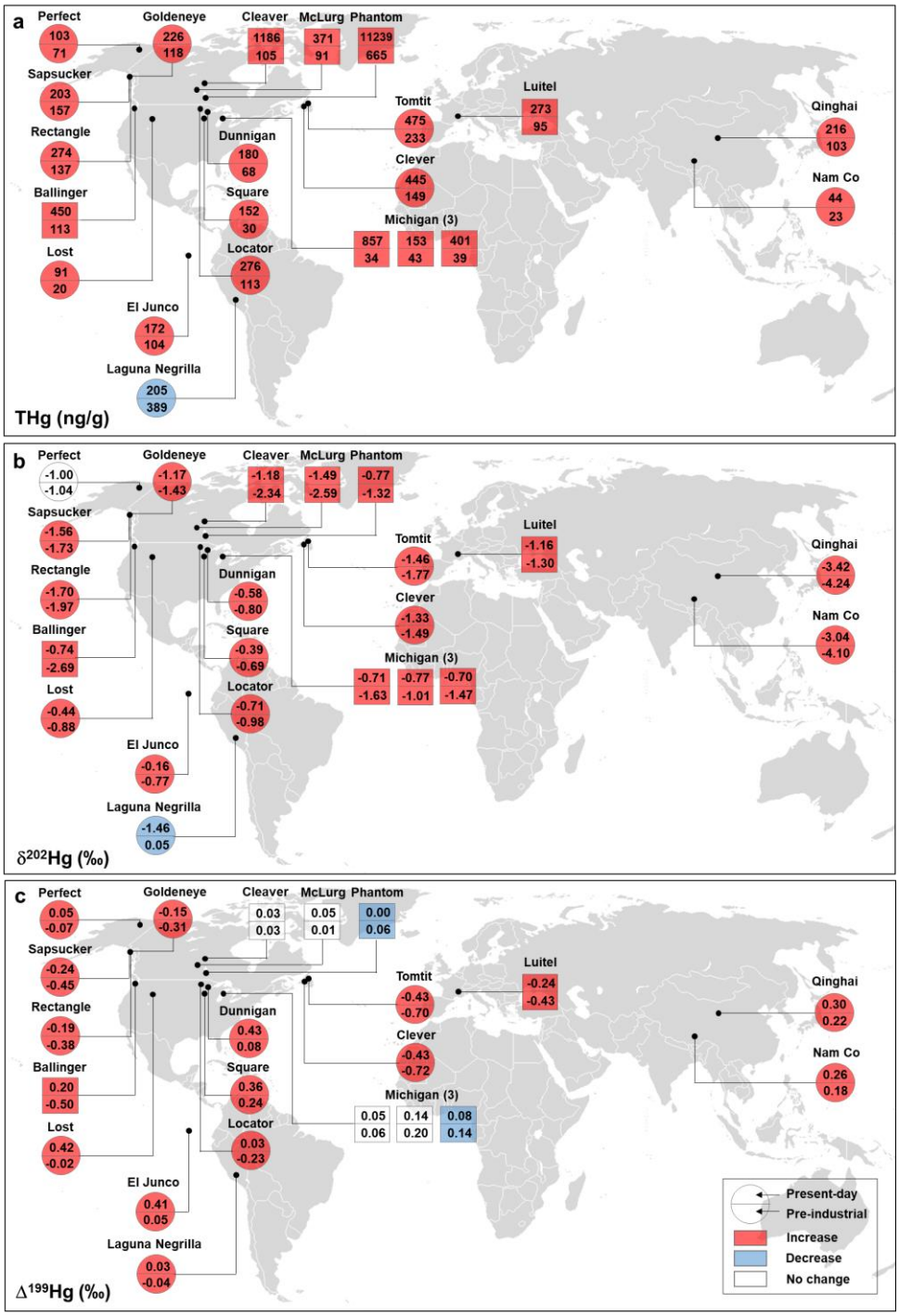


**Figure 1.** Spatiotemporal changes in a) THg concentration (ng/g), b) $\delta^{202}$Hg (‰), and c) $\Delta^{199}$Hg (‰) from the pre-industrial to present-day period in all lake sediment cores. The sediment cores shown in circles represent remote sites and the sediment cores in squares represent unremote sites.

To understand the spatial difference in the magnitude of THg concentration change, we compared the magnitude of THg change between the pre-industrial and present-day period and observed a wide range across the sites (0.53- to 25-fold increase; Figure 1a). For present-day samples, significantly higher THg concentrations were observed in the unremote lakes (median; 620±4140 ng/g, range; 127-19076 ng/g, n = 47) compared to the remote sediments (median; 192±104 ng/g, range; 38-497 ng/g, n = 56, Kruskal-Wallis test, $p < 0.05$, Table S5). The present-day unremote sediments showed 2.9- to 25-fold increases in THg relative to their respective pre-industrial sediments. The present-day remote sediments, without Laguna Negrilla, Peru, showed 1.3- to 5.1-fold increases in THg, consistent with those reported from other lake sediment cores collected from remote regions (3-5 fold) (Amos et al., 2015; Engstrom et al., 2014; Fitzgerald et al., 2005, Li et al., 2020). Among the remote sediments, a reduction in THg (0.53-fold) was observed in Laguna Negrilla, Peru (Figure 1a), consistent with the cessation of widespread historical mercury mining for pigment and precious metal extraction (1532-1821 AD) (Cooke et al., 2013). Without Laguna Negrilla, Peru, relatively small increases in THg (1.1- to 2.1-fold increase) were observed in the Tibetan Plateau, China, Alaska, U.S., and the Peruvian Andes, Educador, which are some of the least urbanized and industrialized locations in the world. Higher increases in THg (2.0- to 5.1-fold) and those comparable with the unremote sediments were detected from the Western (Wyoming) and Midwest, U.S. (Wisconsin, Minnesota) and Newfoundland, Canada, suggesting that these locations may be influenced by the transport of regional anthropogenic mercury sources. Our results suggest that the spatial difference in the magnitude of THg increase is governed by the proximity to local and regional anthropogenic mercury sources.

Consistent with the changes in THg, the present-day sediments showed statistically higher mercury isotope ratios ($\delta^{202}$Hg, $\Delta^{199}$Hg, $\Delta^{200}$Hg) compared to the pre-industrial sediments (Kruskal-Wallis test, all $p < 0.05$, Table S5, Figure 1, Figure 2). The average $\delta^{202}$Hg and $\Delta^{199}$Hg of the pre-industrial sediments were -1.55±0.96‰ (-5.04 to 0.37‰, n = 138) and -0.15±0.28‰ (-0.79 to 0.29‰, n = 138), respectively. Only seventeen out of twenty-two cores reported $\Delta^{200}$Hg (Figure S2), which showed an average value of 0.03±0.07‰ (-0.09 to 0.23‰, n = 122). The average $\delta^{202}$Hg, $\Delta^{199}$Hg, and $\Delta^{200}$Hg of the present-day sediments were -1.07±0.69‰ (-3.68 to -0.16‰, n = 100), 0.07±0.22‰ (-0.44 to 0.48‰, n = 100), and 0.06±0.06‰ (-0.03 to 0.20‰, n = 78), respectively. The magnitude of changes in mercury isotope ratios varied widely across geographic locations (Figure 1b, c). Even within a single lake, Lake Michigan, the magnitude of changes in mercury isotope ratios from the pre-industrial to present-day period were highly variable. This suggests that, unlike THg, the magnitude of changes in mercury isotope ratios are not determined by the proximity to anthropogenic mercury sources, which we discuss further in the section below (3.3). Among the present-day sediments, the remote sediments displayed statistically higher $\Delta^{200}$Hg (Kruskal-Wallis test, $p < 0.05$, Table S5), but not $\delta^{202}$Hg ($p = 0.77$) and $\Delta^{199}$Hg ($p = 0.06$), compared to the unremote sediments. The average $\Delta^{200}$Hg of the remote and unremote sediments were 0.09±0.07‰ (n = 46) and 0.02±0.03‰ (n = 32), respectively (Figure 2c). The unremote sediments were characterized by a narrow range in $\delta^{202}$Hg (-0.93±0.31‰, n = 52) and were statistically similar with the remote sediments, which had a wider range in $\delta^{202}$Hg (-1.21±0.93‰, n = 48, Figure 2a). Both the unremote (0.03±0.11‰, n = 52) and remote sediments (0.12±0.29‰, n = 48) showed near-zero $\Delta^{199}$Hg (Figure 2b).

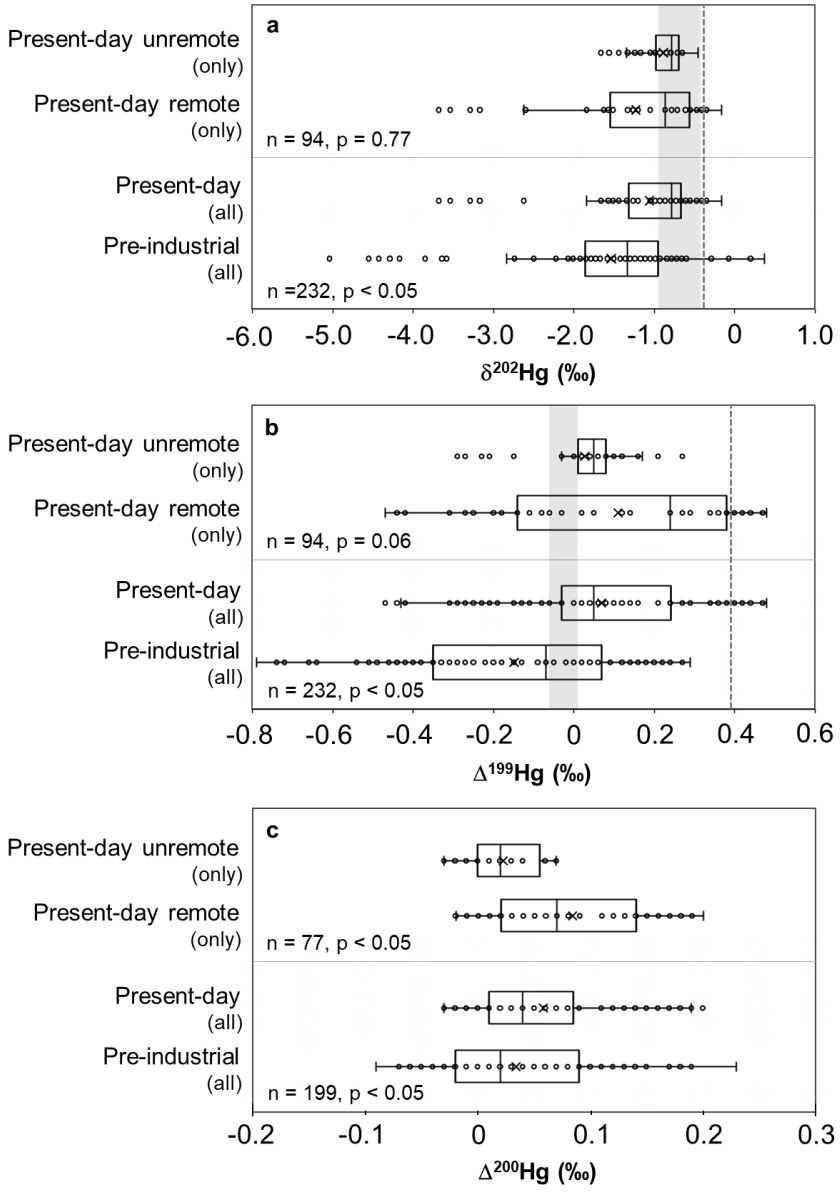


**Figure 2.** The ranges of a) $\delta^{202}$Hg (‰), b) $\Delta^{199}$Hg (‰), and c) $\Delta^{200}$Hg (‰) of the pre-industrial and present-day sediments. The present-day sediments are further divided into remote and unremote. The shaded areas represent the ranges of modern-day $\delta^{202}$Hg (-0.94 to -0.44‰) and $\Delta^{199}$Hg (-0.07 to 0.01‰) of anthropogenic THg emission source end member estimated by Sun et al. (2016). The dotted lines represent the median $\delta^{202}$Hg (-0.38‰) and $\Delta^{199}$Hg (0.39‰) of precipitation compiled by Kwon et al. (2020).

The mercury isotope ratios of the pre-industrial sediments appear to reflect both natural and anthropogenic mercury delivered via atmospheric deposition and runoff from the adjacent watershed. Previous evaluations of anthropogenic mercury enrichments in sediment and peat cores have suggested that historical anthropogenic activities (since 1450 AD) such as Spanish colonial mercury and silver mining (Amos et al., 2015) as well as deforestation and biomass combustion (Li et al., 2020) have liberated substantial amounts of mercury into the atmosphere. The resultant $Hg^0$ would have accumulated within foliage prior to watershed runoff or deposited to lake sediments upon atmospheric oxidation. Sun et al. (2016), who estimated the isotopic end members for anthropogenic mercury emission sources, suggested that historical anthropogenic mercury emissions (~1850s), originated via mining and liquid mercury use in gold and silver refining processes, have ranges of median $\delta^{202}Hg$ of -1.19 to -1.10‰ (THg, $Hg^0$, $Hg^{2+}$, $Hg_P$), which are similar to the pre-indsutrial sediment $\delta^{202}Hg$ compiled here but much lower than those estimated for modern-day anthropogenic mercury emission sources. The estimated $\Delta^{199}Hg$ are similar between the historical (-0.05 to -0.02‰) and modern-day anthropogenic mercury emission sources (-0.06 to -0.02‰; Sun et al., 2016). The atmospheric deposition of both natural and historical anthropogenic mercury emission sources, together with watershed runoff of $Hg^0$ sequestered in foliage, which is known to cause measurable negative $\delta^{202}Hg$ shifts in foliage relative to atmospheric $Hg^0$ (Demers et al., 2013), would explain the low $\delta^{202}Hg$ in the pre-industrial sediments. As for $\Delta^{199}Hg$, the influence of terrestrial mercury sources (soil, litterfall), characterized by negative $\Delta^{199}Hg$ (-0.49 to -0.14‰; Demers et al., 2013; Jiskra et al., 2015, 2017), also explain the low $\Delta^{199}Hg$ in the pre-industrial sediments.

The significantly higher THg and mercury isotope ratios observed in the present-day sediments compared to the pre-industrial sediments can be explained by the influence of modern-day anthropogenic mercury emission sources. Anthropogenic emissions of $Hg^{2+}$ and $Hg_P$, which readily deposit to lakes relative to $Hg^0$, have increased in the modern-day period owing to the activities in by-product sectors (i.e., fossil fuel combustion) (Sun et al., 2016). Sun et al. (2016) estimated significantly higher $\delta^{202}Hg$ in the modern-day (~2010s) anthropogenic THg emission sources (median $\delta^{202}Hg$; -0.70‰, range; -0.94 to -0.44‰) relative to the pre-industrial anthropogenic emissions and the average pre-industrial sediment $\delta^{202}Hg$ compiled in this study. The median $\delta^{202}Hg$ (-0.84‰) reflecting modern-day anthropogenic $Hg^{2+}$ and $Hg_P$ emissions also showed similar estimated values relative to THg (Sun et al., 2016). The anthropogenic mercury emission source end members estimated by Sun et al. (2016) are relatively similar with the average $\delta^{202}Hg$ and $\Delta^{199}Hg$ of the present-day unremote sediments impacted by anthropogenic activities and those that displayed narrow ranges in $\delta^{202}Hg$ and $\Delta^{199}Hg$ (Figure 2a, b). Precipitation samples influenced by varying degrees of anthropogenic mercury emission sources and those recently compiled by Kwon et al. (2020) also show higher $\delta^{202}Hg$ (median -0.38‰; -4.27 to 0.31‰, n = 122) and particularly high $\Delta^{199}Hg$ (median 0.39‰; -0.87 to 1.57‰, n = 122) compared to the average pre-industrial sediments. Given the ~4-fold increase in the global atmospheric mercury deposition since industrialization (Amos et al., 2015), it is likely that the widespread anthropogenic activities have increased the amount of mercury available for deposition to lake sediments even at remote sites. This explains the absence of significant differences in $\delta^{202}Hg$ and $\Delta^{199}Hg$ between the present-day remote and unremote sediments. Moreover, even with the modern-day increase in $Hg^0$ available for foliar uptake and runoff to lake sediments, the estimated higher $\delta^{202}Hg$ of $Hg^0$ in the modern-day anthropogenic mercury emission sources (median; -0.56‰) relative to historical

anthropogenic mercury emission sources (median; -1.12‰) (Sun et al., 2016) may explain the overall $\delta^{202}$Hg increase in the present-day sediment.

In regards to $\Delta^{200}$Hg, a recent study by Lepak et al. (2020b) suggested that the spatial variability in $\Delta^{200}$Hg among remote lake sediments is driven by the relative contribution of atmopsheric (precipitation $Hg^{2+}$) versus watershed (foliage $Hg^0$) mercury sources (Lepak et al., 2020b). While this may be the case for our present-day remote sediments, the significantly higher $\Delta^{200}$Hg observed in the present-day remote sediments relative to the unremote sediments (Figure 2c) may be explained by a higher extent of mercury photo-oxidation prior to deposition. The lakes designated as remote in this study are located far from local anthropogenic mercury emissions sources, as suggested by the individual authors, and receive mercury that has been subjected to regional transport. The $\Delta^{200}$Hg has been used as a conservative tracer to evaluate the relative importance of precipitation derived mercury input to surface reservoirs and/or the extent of atmospheric mercury photo-oxidation (Blum & Johnson, 2017). Here, we compiled wet mercury deposition fluxes from Lepak et al. (2020a), who reported measured fluxes to nine remote lakes in North America and those compiled here, and from Mulvaney et al. (2020), who simulated a global atmospheric chemistry transport model for mercury (GEOS-Chem; Table S6). There was no significant difference in wet mercury deposition fluxes between the remote and unremote lakes (Kruskal-Wallis test, $p < 0.05$), indicating that the extent of precipitation derived mercury input is not responsible for the $\Delta^{200}$Hg difference between the remote and unremote sediments. The watershed area to lake area ratio, an indicator for the relative input of atmospheric ($Hg^{2+}$) versus watershed mercury ($Hg^0$) input, also showed no clear differences between the remote and unremote lakes (Table S6). We speculate that a higher extent of $Hg^0$ photo-oxidation, resulting in a higher

$\Delta^{200}$Hg and a lower $\delta^{202}$Hg in $Hg^{2+}$ compared to $Hg^0$ (Cai & Chen, 2016), during regional transport prior to deposition may explain the significantly higher $\Delta^{200}$Hg and slightly lower $\delta^{202}$Hg observed in the remote sediments compared to the unremote sediments.

As for the present-day remote sediments, the relative contribution of atmospheric versus watershed mercury sources appears to explain the spatial variability in $\Delta^{200}$Hg. We observed significantly higher $\delta^{202}$Hg (-0.54±0.16‰), $\Delta^{199}$Hg (0.28±0.19‰), and $\Delta^{200}$Hg (0.13±0.05‰) in five lakes (Dunnigan and Square, Minnesota, Locator, Wisconsin, Lost, Wyoming in the U.S., El Junco, Peru; Figure 1b, c, Figure S2), characterized by high wet mercury deposition fluxes and small watershed area to lake area ratios, compared to other remote lakes compiled in this study ($\delta^{202}$Hg; -1.94±0.87‰, $\Delta^{199}$Hg; -0.07±0.28‰, $\Delta^{200}$Hg; 0.03±0.03‰, Kruskal-Wallis test, all $p < 0.05$, Table S5). Lepak et al. (2020b) reported higher wet mercury deposition fluxes (7.7 to 9.4 $\mu g/m^2/yr$) coupled with small watershed area to lake area ratios (2.0 to 8.2) in Dunnigan, Locator, and Square compared to other remote lakes in North America (wet mercury deposition fluxes; 1.5 to 4.6 $\mu g/m^2/yr$, watershed area to lake area ratios; 1.2 to 13). The present-day wet mercury deposition fluxes simulated by GEOS-Chem and those reported by Mulvaney et al. (2020) also show much higher values (8.2 to 12 $\mu g/m^2/yr$) and small watershed area to lake area ratios (2.1 to 2.2) in El Junco and Lost compared to other remote lakes (Table S6). All in all, our compilation study suggests that mercury isotope ratios in lake sediment cores can be used to evaluate the large-scale influence of modern-day anthropogenic mercury emission sources as well as the relative importance of mercury input pathways (atmospheric versus watershed runoff) across remote regions. While further study is required to verify processes affecting mercury isotope ratios in the

atmosphere prior to deposition to lake sediments, we suggest that sediment $\Delta^{200}$Hg may be used to gain insights into the influence of local versus regional anthropogenic mercury deposition.

### 3.2 Sources & processes governing temporal changes

Results from the conventional linear trend test show widespread increasing trends of THg and mercury isotope ratios in the lake sediment cores from the pre-industrial to present-day period. Most of the sediment cores showed a statistically significant increasing linear trend in THg with the 95% confidence level (p value $\leq$ 0.05; Table S4) while one lake sediment show a significant decreasing trend in THg (Laguna Negrilla). Based on the analytical uncertainty estimates, significant positive shifts in $\delta^{202}$Hg (>2SD of 0.09‰) were observed in 20 sediment cores from the pre-industrial to present-day period, except for Perfect Lake in the Arctic (Lepak et al., 2020b) and Laguna Negrilla, Peru (Cooke et al., 2013) (Figure 1b). Sixteen and three lake sediment cores showed a significant positive shift in $\Delta^{199}$Hg (> 2SD of 0.06‰) and $\Delta^{200}$Hg (> 2SD of 0.05‰), respectively (Figure 1c, Figure S2). According to the linear trend test, 17 out of 22 lake sediment cores showed a statistically significant increasing trend in $\delta^{202}$Hg at the 95% confidence level (p value $\leq$ 0.05; Table S4). Fifteen lake sediment cores showed significant positive temporal trends in $\Delta^{199}$Hg at the 95% confidence level and two cores showed significant negative trends in $\Delta^{199}$Hg (Table S4). Overall, our results suggest that, in addition to $\Delta^{199}$Hg, the positive shifts in THg concentration together with $\delta^{202}$Hg are widespread phenomena across the lake sediment cores.

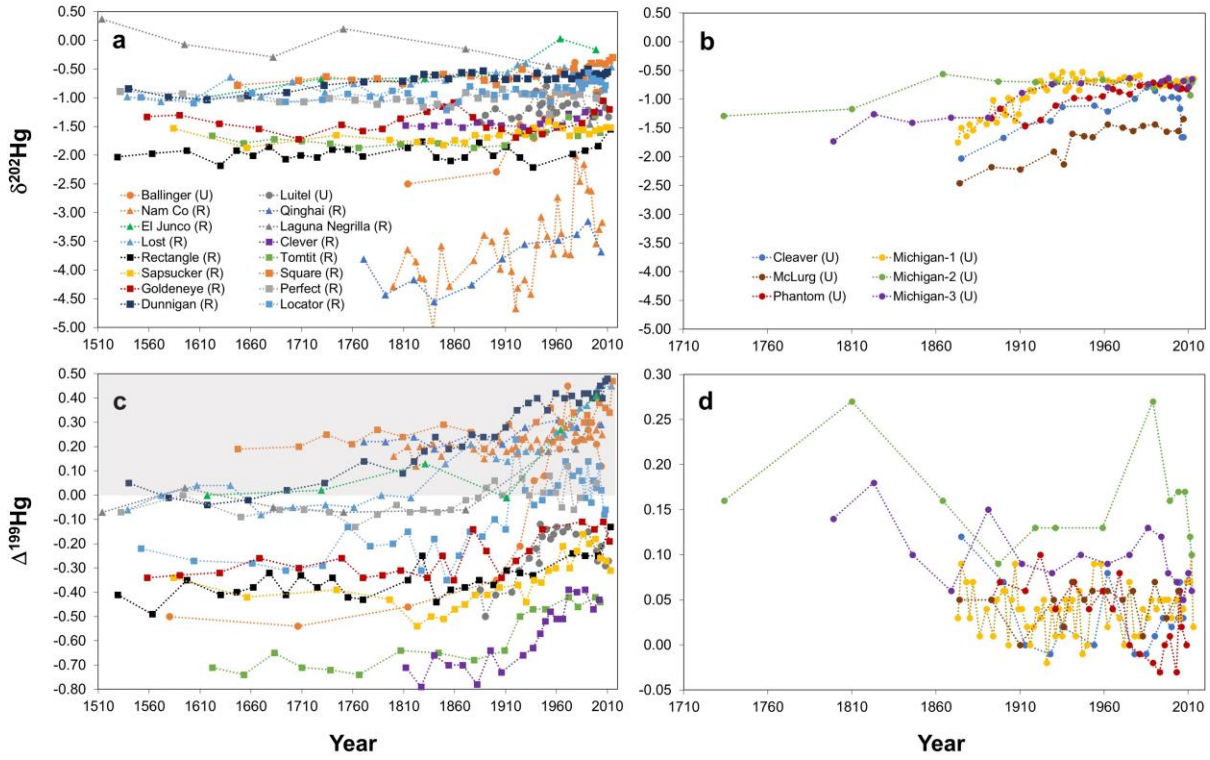


**Figure 3.** Temporal trends in $\delta^{202}$Hg (a, b) and $\Delta^{199}$Hg (c, d) of all lake sediment cores. The lake sediment cores designated as U and R indicate unremote and remote, respectively. The shaded area in panel c represents sediment cores (Nam Co, Qinghai in Tibet, Dunnigan, Square in Minnesota, U.S.), which exhibited positive $\Delta^{199}$Hg shifts even with elevated $\Delta^{199}$Hg baselines. Panel d represents sediment cores that showed no significant shifts in $\Delta^{199}$Hg (Cleaver, McLurg in Manitoba, Canada, two locations in Lake Michigan) and sediment cores that had significant negative $\Delta^{199}$Hg shifts (Phantom in Manitoba, Canada, one location in Lake Michigan).

### 3.2.1 $\delta^{202}$Hg

The widespread positive $\delta^{202}$Hg shifts from the pre-industrial to present-day period appear to be caused by increased contribution of modern-day anthropogenic mercury emission sources, which are characterized by a higher $\delta^{202}$Hg compared to the pre-industrial sediments. Among the

sediment cores compiled in this study, we observed significant negative relationships between $\delta^{202}$Hg and 1/THg ($p < 0.05$, $r^2 = 0.21$ to 0.93), except for three lakes in North America (Goldeneye and Rectangle, Alaska, Perfect Lake in the Arctic) and Lake Qinghai, Tibet (Yin et al., 2016a) ($p > 0.05$, $r^2 = 0.03$ to 0.15; Table S7). This suggests that the majority of sediment cores depict an increasing contribution from anthropogenic mercury sources to the pre-industrial sediments, which have low THg and negative $\delta^{202}$Hg (Figure 2).

The significant temporal $\delta^{202}$Hg trends observed in the lake sediment cores further suggest that local to regional anthropogenic mercury emission sources, which share a similar $\delta^{202}$Hg, contribute to the positive $\delta^{202}$Hg shifts. As illustrated in Figure 3, both the remote and unremote lake sediment cores exhibited increasing trends in $\delta^{202}$Hg with temporally corresponding peaks in THg and $\delta^{202}$Hg (Figure 3a, b, Figure S3). The median $\delta^{202}$Hg corresponding to the THg peaks is -0.80±0.92‰, which is within the ranges of precipitation impacted by anthropogenic activities and anthropogenic mercury emission end member estimated by Kwon et al. (2020) and Sun et al. (2016), respectively. An exception was observed in Laguna Negrilla, which had a higher pre-industrial $\delta^{202}$Hg compared to the anthropogenic mercury source end member and exhibited a decreasing temporal trend in THg and $\delta^{202}$Hg, consistent with the cessation of widespread historical mercury mining for pigment and precious metal extraction (Cooke et al., 2013). The measurable reductions in THg concentrations relative to small changes in $\delta^{202}$Hg in the recent decades (Figure 3a, b, Figure S3) may be explained by the absence of significant alterations in mercury sources. Amos et al. (2015), who compiled mercury concentrations in natural archives, also reported peaks in THg during the second half of the 20$^{th}$ century and declines in the recent decades. The authors attributed this to large-scale reductions in anthropogenic mercury emissions

leading to rapid reductions in atmospheric mercury deposition and slow reductions in terrestrial reservoirs, which both supply mercury to lake sediments. Similarly, while the rapid and slow reductions in atmospheric deposition and watershed runoff of mercury may explain the overall declining trends in sediment THg concentrations, the input of constant mercury sources may explain minor changes in $\delta^{202}$Hg.

Based on the similar $\delta^{202}$Hg value between the median anthropogenic mercury emission source end member estimated by Sun et al. (2016) and the average $\delta^{202}$Hg of the present-day unremote sediments, we speculate that processes affecting mercury in the atmosphere and within a lake system play minor roles in modifying $\delta^{202}$Hg of anthropogenic mercury emission sources. While many processes are known to result in significant MDF (Blum et al., 2014; Kwon et al., 2020), previous studies have suggested that lake sediment cores are less prone to diagenetic and hydrodynamic effects resulting in mercury mobility and release compared to other natural archives (i.e., peat, marine sediment cores) (Asmund & Nielsen, 2000; Cooke et al., 2020; Wasik et al., 2015). This is supported by the studies that showed consistency in the levels and temporal trends in mercury in lake sediment cores, which have been collected at the same location in different periods (Percival & Outridge, 2013; Rydberg et al., 2008). A recent modeling study of mercury isotopes within a lake system also simulated small to negligible $\delta^{202}$Hg changes in mercury input sources in the sediment during water column and diagenetic processes (Bessinger, 2014). From a temporal perspective, if changes in atmospheric and water column processes were significant enough to cause positive temporal trends in $\delta^{202}$Hg, THg concentrations in the sediments would decrease, which is not what we observed. Experiments have shown that photo-reduction of $Hg^{2+}$ and evaporation of $Hg^0$ result in a higher $\delta^{202}$Hg in the remaining solution compared to the product

(Bergquist & Blum, 2007, Estrade et al., 2009, Ghosh et al., 2013). Increased $Hg^{2+}$ photo-reduction in precipitation or in the water column would reduce the amount of mercury available for deposition to sediments. While increased mercury sorption to particles either in the atmosphere or in the water column may increase sediment THg, an experimental study by Wiederhold et al. (2010) reported a lower $\delta^{202}Hg$ in mercury bound to particles compared to those unbound in solution. We suggest that the increased contribution of modern-day anthropogenic mercury emission sources to the pre-industrial sediments explains the widespread $\delta^{202}Hg$ and THg shifts rather than temporal changes in processes affecting mercury in the atmosphere or within a lake system.

3.2.2 $\Delta^{199}Hg$

In contrast to the previous argument that the positive $\Delta^{199}Hg$ shifts from pre-industrial to present-day period are a global phenomenon, the significant positive shifts were observed in a subset of lake sediment cores compiled in this study. Kurz et al. (2019) provided three hypotheses to explain the positive $\Delta^{199}Hg$ shifts observed in a remote lake sediment core from Wyoming, U.S.; 1) changes in the global atmospheric chemical composition, 2) changes in local processes including increased $Hg^{2+}$ photo-reduction in the water column, and 3) increased anthropogenic mercury source contribution to lake sediments, which have more positive $\Delta^{199}Hg$ compared to geogenic sources. We propose a modified scenario from the latter in which the increased contribution of anthropogenic mercury emission sources is responsible for the positive $\Delta^{199}Hg$ shifts and the significant positive shifts are detected primarily in lake sediments with low pre-industrial $\Delta^{199}Hg$.

We observed significant increasing temporal trends in $\Delta^{199}$Hg in all remote (n = 13) and some unremote lake sediment cores (n = 2) (Figure 3c). Most of these lake sediment cores were characterized by negative pre-industrial $\Delta^{199}$Hg (average -0.38‰, -0.72 to -0.02‰, n = 10) relative to the anthropogenic mercury emission source end member (Sun et al., 2016) and precipitation (Kwon et al., 2020), which have near-zero and positive $\Delta^{199}$Hg, respectively. Seven lake sediment cores, characterized as unremote and near-zero and small positive pre-industrial $\Delta^{199}$Hg (average 0.08‰, 0.01 to 0.20‰), showed no significant and significant reduction in temporal trends in $\Delta^{199}$Hg, respectively (Figure 3d). It is possible that the higher extent of $Hg^{2+}$ photo-reduction within the water column, resulting in a higher $\Delta^{199}$Hg in the remaining mercury relative to $Hg^0$ (Bergquist & Blum, 2007), may explain the small positive $\Delta^{199}$Hg in these sediments. Alternatively, the pre-industrial unremote sediments with near-zero $\Delta^{199}$Hg reflect local anthropogenic mercury sources. We note, however, that the pre-industrial unremote sediments had similarly low THg concentration (average 187 ng/g, 30-941 ng/g) compared to the remote sediments (average 147 ng/g, 18-684 ng/g, Figure 1a). While it is difficult to identify sources and/or processes resulting in more elevated $\Delta^{199}$Hg in certain pre-industrial unremote sediments relative to others, the mixing between two similar end members (near-zero to positive pre-industrial versus anthropogenic $\Delta^{199}$Hg) appears to be responsible for the absence of significant temporal $\Delta^{199}$Hg trends in certain sediment cores.

While only a few processes are known to cause significant MIF (Blum et al., 2014; Kwon et al., 2020), large global environmental changes may have contributed partly to the temporal shifts in $\Delta^{199}$Hg. Previous studies have collectively suggested that, on a global basis, the amount of precipitation has increased significantly since the early 1900s (Ren et al., 2013). This observation

is, however, in contrast with the absence of widespread and significant temporal modifications in $\Delta^{200}$Hg (> 2SD of 0.05‰). On a local scale, the effects of gradual and dramatic changes such as the ice cover and erosional and land-use change may lead to positive temporal shifts in $\Delta^{199}$Hg. In fact, several exceptions were observed in Tibetan lakes (Qinghai, Nam Co), and Dunnigan and Square in Minnesota, which showed increasing temporal $\Delta^{199}$Hg trends even with positive pre-industrial $\Delta^{199}$Hg (average; 0.15‰, 0.05 to 0.24‰; Figure 3c). In Tibetan lakes, Yin et al. (2016a) observed highly negative $\delta^{202}$Hg, similar to terrestrial sources (Demers et al., 2013; Jiskra et al., 2015, 2017), and positive $\Delta^{199}$Hg in the sediments, which then increased over time (Figure 3d). The authors suggested that mercury introduced via watershed runoff was subjected to a higher degree of photo-reduction in the water column with declining ice cover. As such, the fact that the changes in local sources and/or processes may result in significant temporal trends in $\Delta^{199}$Hg in certain lake sediments suggests that the positive $\Delta^{199}$Hg shifts are unlikely to be a global phenomenon. Instead, the widespread and significant positive $\delta^{202}$Hg shifts observed in the lake sediment cores indicate that $\delta^{202}$Hg can serve as an important proxy for assessing temporal changes in anthropogenic mercury source contribution.

### 3.3 Importance of baseline mercury isotope ratios

The evaluation of the temporal trends in the lake sediment cores indicates that the increased contribution of local to regional anthropogenic mercury emission sources, which have a similar $\Delta^{199}$Hg and a much higher $\delta^{202}$Hg compared the pre-industrial sediments, explain the differences in the temporal trends between $\delta^{202}$Hg and $\Delta^{199}$Hg. While the negative pre-industrial $\delta^{202}$Hg resulted in the widespread positive shifts in $\delta^{202}$Hg, the near-zero pre-industrial $\Delta^{199}$Hg resulted in either absence or small positive shifts in $\Delta^{199}$Hg in the lake sediment cores. To further evaluate the

importance of pre-industrial mercury isotope ratios for explaining the temporal trends, we estimate the magnitude of $\delta^{202}$Hg and $\Delta^{199}$Hg changes from the pre-industrial to the present-day period except for Laguna Negrilla, which decreased in THg. In this assessment, the average sediment mercury isotope ratios reflecting the pre-industrial period are set as baseline or a starting point of each core and the sediment $\delta^{202}$Hg and $\Delta^{199}$Hg for each dated year are subtracted from the average pre-industrial $\delta^{202}$Hg and $\Delta^{199}$Hg (baseline) to quantify the magnitude of changes in mercury isotope ratios over time. As illustrated in Figure 4, the lake sediment cores with the most negative $\delta^{202}$Hg (-4.24 to -2.34‰) and $\Delta^{199}$Hg baselines (-0.72 to -0.43‰) increased dramatically in $\delta^{202}$Hg (by 0.82 to 1.95‰) and $\Delta^{199}$Hg (by 0.20 to 0.70‰) in the present-day period. The magnitude of $\delta^{202}$Hg and $\Delta^{199}$Hg increases from the baseline to the present-day period decreased as the baseline $\delta^{202}$Hg and $\Delta^{199}$Hg increased in each sediment core. Moreover, we found that the magnitude of $\delta^{202}$Hg and $\Delta^{199}$Hg changes did not correlate with the magnitude of THg changes ($\delta^{202}$Hg; $r^2$ = 0.09, $\Delta^{199}$Hg; $r^2$ = 0.20, both $p > 0.05$). Even among the unremote ($\delta^{202}$Hg; $r^2 < 0.01$, $\Delta^{199}$Hg; $r^2$ = 0.17, both $p > 0.05$) and remote sediments ($\delta^{202}$Hg; $r^2 < 0.01$, $\Delta^{199}$Hg; $r^2 = 0.07$, both $p > 0.05$), we did not observe significant relationships between the magnitude of $\delta^{202}$Hg and $\Delta^{199}$Hg changes and the magnitude of THg changes. This indicates that, unlike the THg concentration, the magnitude of mercury isotope ratio changes are not governed by the extent of mercury input.

Our results are in contrast with Lepak et al. (2020b), who observed significant positive relationships between the magnitude of changes in mercury accumulation flux, which is correlated with the sediment THg concentration, and the magnitude of changes in $\delta^{202}$Hg and $\Delta^{199}$Hg in nine remote lake sediments of North America. In that study, the authors suggested that the differences in the amount of atmospheric mercury input sourced from precipitation determines the inter-lake

variability in the magnitude of mercury isotope ratio changes over time. Our compilation of twenty-two lake sediment cores suggests that the magnitude of changes in mercury isotope ratios from the pre-industrial to present-day period is governed by the pre-industrial variability in mercury isotope ratios. Even among the remote and unremote sediments, which showed drastic differences in their magnitude of THg change, the present-day mercury isotope ratios were statistically similar, supporting our conclusion that the changes in mercury isotope ratios in lake sediment cores reflect isotope mixing between anthropogenic mercury emission sources and pre-industrial sediments. Based on the isotope mixing effect, we expect that further increase in the contribution of anthropogenic mercury emission sources to lake sediments would lead to cessation of further shifts in sediment mercury isotope ratios, while mercury concentration continues to increase via the input. Even within a single lake, Lake Michigan, Yin et al. (2016b) observed differences in the pre-industrial sediment mercury isotope ratios across three sites ($\delta^{202}$Hg = -1.63 to -1.01‰, $\Delta^{199}$Hg = 0.06 to 0.20‰), and the magnitude of changes from the pre-industrial to present-day period ($\delta^{202}$Hg; by 0.24 to 0.92, $\Delta^{199}$Hg; by 0.01 to 0.06; Figure 1b, c) did not correlate with the magnitude of THg changes. This indicates that either within a single lake or across multiple lakes, the baseline $\delta^{202}$Hg and $\Delta^{199}$Hg play a more important role in determining the magnitude of changes in mercury isotope ratios compared to THg.

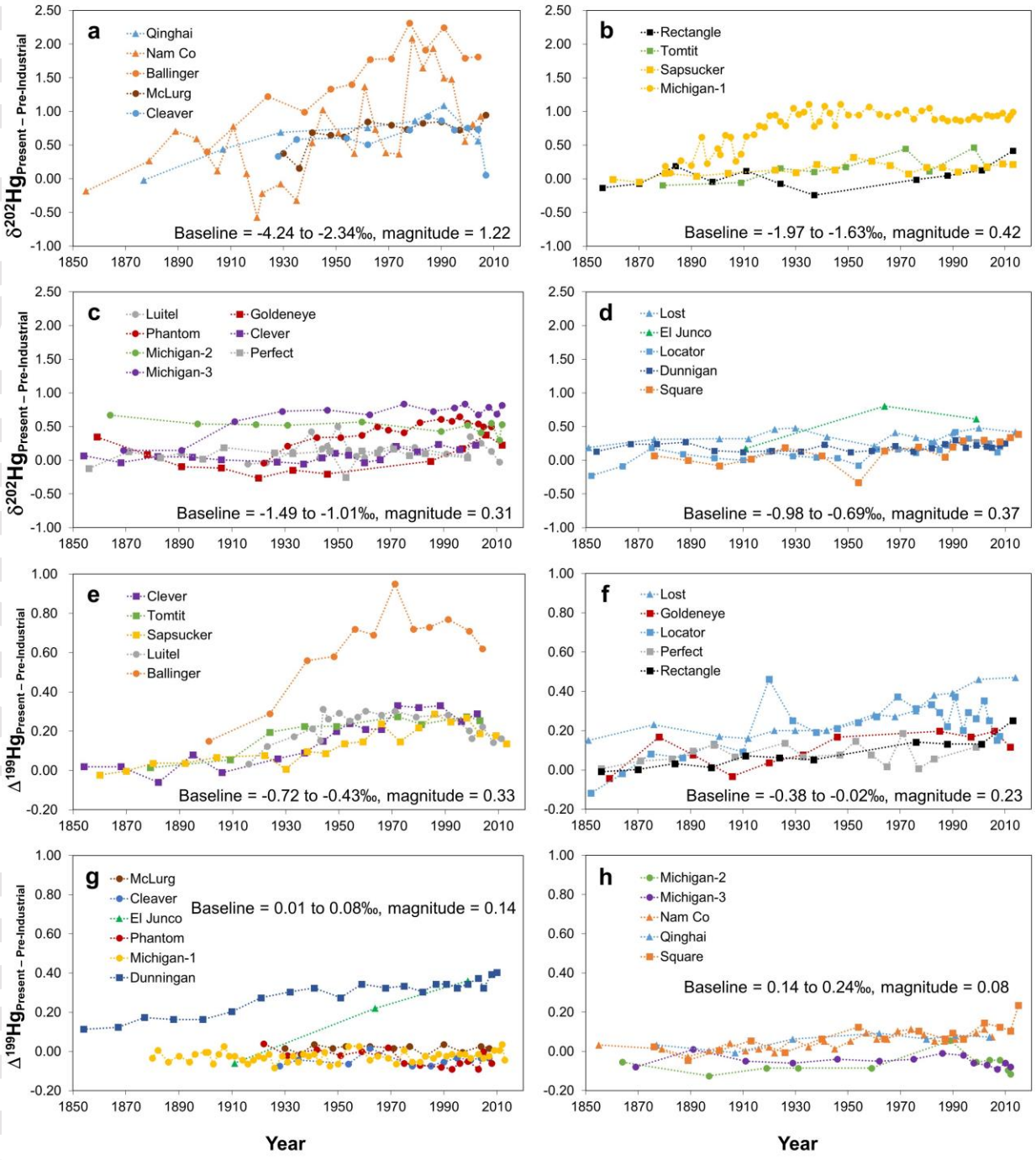


**Figure 4.** Magnitude of $\delta^{202}$Hg (a to d) and $\Delta^{199}$Hg changes (e to h) from the pre-industrial (1510-1850) period to the next core interval over time. From each panel, baseline represents the ranges

of the pre-industrial $\delta^{202}$Hg or $\Delta^{199}$Hg. Magnitude indicates the average magnitude of $\delta^{202}$Hg or $\Delta^{199}$Hg changes from the pre-industrial to present-day period.

### 3.4 Implication for the Minamata Convention on Mercury

The compilation of mercury isotope ratios in lake sediment cores suggests that $\delta^{202}$Hg and $\Delta^{199}$Hg of anthropogenic mercury emission sources and $\Delta^{200}$Hg reflecting the extent of photo-oxidation are well preserved in lake sediments. In regards to temporal trends, we attribute the widespread positive shifts in $\delta^{202}$Hg in the lake sediment cores (e.g., Guérdron et al., 2016; Lepak et al., 2020b) to local to global rise in the modern-day anthropogenic mercury sources. The absence of widespread shifts in $\Delta^{199}$Hg can be explained by a similar $\Delta^{199}$Hg value between the pre-industrial sediments and modern-day anthropogenic mercury emission sources. The fact that the changes in local sources and/or processes may result in temporal trends in $\Delta^{199}$Hg in certain lake sediments suggests that the positive $\Delta^{199}$Hg shifts are unlikely to be a global phenomenon. While $\Delta^{199}$Hg has been regarded as a conservative tracer for mercury sources due to limited processes resulting in MIF, our results suggest that the temporal evaluation of $\delta^{202}$Hg, which has a much higher value compared to the pre-industrial sediments, is a more powerful proxy for evaluating long-term changes in anthropogenic mercury sources. Across a broad spatial scale, the characterization of pre-industrial mercury isotope ratios will be critical for deciphering between the absence and significant changes in mercury isotope ratios resulted from anthropogenic mercury source contribution.

Our study has wide-ranging implications for the global monitoring and effectiveness evaluation of the MC. Many previous studies have assessed temporal trends in mercury using

atmospheric samples (Cheng et al., 2017; Dommergue et al., 2016) and biota (Blukacz-Richards et al., 2017; Lee et al., 2016; McKinney et al., 2017). While these samples provide insights into rapid responses to changes in mercury emissions and bioaccumulation, the isotope ratios reflecting mercury sources are susceptible to change via environmental, biological, and ecological conditions. For instance, previous studies have observed large seasonal and air mass differences in mercury isotope ratios in atmospheric samples (Fu et al., 2016; Huang et al., 2018). The tissues of biota including fish and birds have shown measurable MDF in the bioaccumulated mercury sources caused by metabolic processes (Kwon et al., 2013). The mercury isotope ratios of biota tissues also reflect a mixture of mercury sources, which may have been integrated over time and space (i.e., migratory sites) (Renedo et al., 2018, 2021). In fact, deciphering between policy signal and environmental noise has been one of the greatest challenges of evaluating the effectiveness of the MC. In this regard, the effective and long-term preservation of mercury isotope ratios of anthropogenic mercury sources in lake sediment cores can serve as an important proxy for assessing changes in anthropogenic mercury sources. The information on the pre-industrial mercury isotope ratios can also serve as an ideal and site-specific target for the effectiveness evaluation of the MC in which the large-scale reduction in local to regional anthropogenic mercury emissions would allow sediment mercury isotope ratios to recover to values similar to the pre-industrial sediment values. Lastly, when predicting future changes in mercury isotope ratios in sediment cores, the types of mercury emitting sectors governed under the MC and modifications in mercury abatement technologies need to be considered. The intentional mercury use sectors including mining and manufacturing of commercial products, which predominantly emit $Hg^0$, are subject to the most stringent global regulation (UNEP, 2019). Dramatic reductions in $Hg^0$, which have the highest $\delta^{202}Hg$ relative to $Hg^{2+}$ and $Hg_P$ based on the anthropogenic mercury source end

members estimated by Sun et al. (2016), may suppress further increases in $\delta^{202}$Hg in sediment cores. The types of mercury abatement technologies in by-product sectors (i.e., fossil fuel combustion) are also known to determine $\delta^{202}$Hg of the emitted mercury (Sun et al., 2014). We suggest that future studies that assess the timescale of mercury isotope turnover in relation to reduction of anthropogenic mercury input and the sensitivity of local to global environmental and policy changes would enhance the utility of mercury isotopes measured in sediments for the monitoring and effectiveness evaluation of the MC.


## Acknowledgments

This work was supported by the National Research Foundation of Korea (NRF) funded by the Korea government (MSIT) (NRF-2015M1A5A1037243, NRF-2019R1F1A1058928, NRF-2020R1A4A1018818, NRF-2021R1C1C1008429), the research program of the Korea Institute of Ocean Science and Technology (KIOST) (PE99883) and Korea Polar Research Institute (KOPRI) (PN20090). The authors declare no conflicts of interest.


## Data Availability Statement

The compiled data used in this study is available at https://doi.org/10.5281/zenodo.5077887 (or https://github.com/jhl329/lake-sediment-cores_compiled-data).

## References


Amos, H. M., Sonke, J. E., Obrist, D., Robins, N., Hagan, N., Horowitz, H. M., Mason, R. P., Witt, M., Hedgecock, I. M., Corbitt, E. S. & Sunderland, E. M. (2015). Observational and

modeling constraints on global anthropogenic enrichment of mercury. *Environmental Science and Technology, 49*(7), 4036-4047. https://doi.org/10.1021/es5058665

Appleby, P. G., & Oldfield, F. (1978). The calculation of lead-210 dates assuming a constant rate of supply of unsupported 210Pb to the sediment. *Catena, 5*(1), 1-8. https://doi.org/10.1016/S0341-8162(78)80002-2

Appleby, P. G., & Oldfield, F. (1992). Applications of lead-210 to sedimentation studies. In Uranium-series disequilibrium: applications to earth, marine, and environmental sciences. 2. ed. Clarendon Press, Oxford.

Appleby, P. G. (2002). Chronostratigraphic techniques in recent sediments. In Tracking environmental change using lake sediments (pp. 171-203). Springer, Dordrecht.

Asmund, G. & Nielsen, S. P. (2000). Mercury in dated Greenland marine sediments. *Science of The Total Environment*, *245*(1-3), 61-72. https://doi.org/10.1016/S0048-9697(99)00433-7

Baskaran, M. (2016). Radon: A tracer for geological, geophysical and geochemical studies (Vol. 367). Basel: Springer.

Benoit, J. M., Gilmour, C. C., Heyes, A., Mason, R. P., & Miller, C. L. (2003). Geochemical and biological controls over methylmercury production and degradation in aquatic ecosystems, *ACS Symposium Series, 835*, 262-297. https://doi.org/10.1021/bk-2003-0835.ch019

Bergquist, B. A. & Blum, J. D. (2007). Mass-dependent and -independent fractionation of Hg isotopes by photoreduction in aquatic systems. *Science*, *318*(5849), 417–420. DOI: 10.1126/science.1148050

Bergquist, B. A., & Blum, J. D. (2009). The odds and evens of mercury isotopes: applications of mass-dependent and mass-independent isotope fractionation. *Elements, 5*(6), 353-357. https://doi.org/10.2113/gselements.5.6.353

Bessinger, B. A. (2014). Use of stable isotopes to identify sources of mercury in sediments: a review and uncertainty analysis. *Environmental Forensics*, *15*(3), 265-280. https://doi.org/10.1080/15275922.2014.930939

Blaauw, M. (2010). Methods and code for 'classical'age-modelling of radiocarbon sequences. *Quaternary Geochronology, 5*(5), 512-518. https://doi.org/10.1016/j.quageo.2010.01.002

Blukacz-Richards, E. A., Visha, A., Graham, M. L., McGoldrick, D. L., de Solla, S. R., Moore, D. J., & Arhonditsis, G. B. (2017). Mercury levels in herring gulls and fish: 42 years of spatio-temporal trends in the Great Lakes. *Chemosphere*, *172*, 476-487. https://doi.org/10.1016/j.chemosphere.2016.12.148

Blum, J. D., & Bergquist, B.A. (2007). Reporting of variations in the natural isotopic composition of mercury. *Analytical and Bioanalytical Chemistry, 388,* 353–359. https://doi.org/10.1007/s00216-007-1236-9

Blum, J. D., Sherman, L. S., & Johnson, M. W. (2014). Mercury isotopes in earth and environmental sciences. *Annual Review of Earth and Planetary Sciences, 42,* 249–269. https://doi.org/10.1146/annurev-earth-050212-124107

Blum, J. D. & Johnson, M. W. (2017). Recent developments in mercury stable isotope analysis. *Reviews in Mineralogy and Geochem*istry, *82*(1), 733-757. https://doi.org/10.2138/rmg.2017.82.17

Cai, H., & Chen, J. (2016). Mass-independent fractionation of even mercury isotopes. *Science Bulletin, 61*(2), 116-124. https://doi.org/10.1007/s11434-015-0968-8

Chen, J., Hintelmann, H., Feng, X., & Dimock, B. (2012). Unusual fractionation of both odd and even mercury isotopes in precipitation from Peterborough, ON, Canada. *Geochimica et Cosmochimica Acta, 90,* 33–46. https://doi.org/10.1016/j.gca.2012.05.005

Cheng, I., Zhang, L., Castro, M., & Mao, H. (2017). Identifying Changes in Source Regions Impacting Speciated Atmospheric Mercury at a Rural Site in the Eastern United States. *Journal of the Atmospheric Sciences, 74*(9), 2937-2947. https://doi.org/10.1175/JAS-D-17-0086.1

Cooke, C. A., Hintelmann, H., Ague, J. J., Burger, R., Biester, H., Sachs, J. P., & Engstrom, D. R. (2013). Use and legacy of mercury in the Andes. *Environmental Science and Technology*, *47*(9), 4181-4188. https://doi.org/10.1021/es3048027

Cooke, C. A., Martínez-Cortizas, A., Bindler, R., & Gustin, M. S. (2020). Environmental archives of atmospheric Hg deposition – A review. *Science of The Total Environment*, *709*, 134800. https://doi.org/10.1016/j.scitotenv.2019.134800

Demers, J. D., Blum, J. D., & Zak, D. R. (2013). Mercury isotopes in a forested ecosystem: Implications for air-surface exchange dynamics and the global mercury cycle. *Global Biogeochemical Cycles*, *27*(1), 222-238. https://doi.org/10.1002/gbc.20021

Dommergue, A., Martinerie, P., Courteaud, J., Witrant, E., & Etheridge, D. M. (2016). A new reconstruction of atmospheric gaseous elemental mercury trend over the last 60 years from Greenland firn records. *Atmospheric Environment*, *136*, 156-164. https://doi.org/10.1016/j.atmosenv.2016.04.012

Eakins, J. A., & Morrison, R. T. (1978). A new procedure for the determination of lead-210 in lake and marine sediments. *The International Journal of Applied Radiation and Isotopes*, *29*(9-10), 531-536. https://doi.org/10.1016/0020-708X(78)90161-8

Engstrom, D. R., Balogh, S. J., & Swain, E. B. (2007). History of mercury inputs to Minnesota lakes: influences of watershed disturbance and localized atmospheric deposition. *Limnology and Oceanography, 52*(6), 2467-2483. https://doi.org/10.4319/lo.2007.52.6.2467

Engstrom, D. R., Fitzgerald, W. F., Cooke, C. A., Lamborg, C. H., Drevnick, P. E., Swain, E. B., Balogh, S. J., & Balcom, P. H. (2014). Atmospheric Hg emissions from preindustrial gold and silver extraction in the Americas: A reevaluation from lake-sediment archives. *Environmental Science and Technology*, *48*(12), 6533-6543. https://doi.org/10.1021/es405558e

Enrico, M., Le Roux, G., Heimbürger, L. E., Van Beek, P., Souhaut, M., Chmeleff, J., & Sonke, J. E. (2017). Holocene atmospheric mercury levels reconstructed from peat bog mercury stable isotopes. *Environment Science and Technology*, *51*(11), 5899-5906. https://doi.org/10.1021/acs.est.6b05804

Estrade, N., Carignan, J., Sonke, J. E., & Donard, O. F. (2009). Mercury isotope fractionation during liquid–vapor evaporation experiments. *Geochimica et Cosmochimica Acta, 73*(10), 2693-2711. https://doi.org/10.1016/j.gca.2009.01.024

Fitzgerald, W. F., Engstrom, D. R., Lamborg, C. H., Tseng, C. M., Balcom, P. H., & Hammerschmidt, C. R. (2005). Modern and historic atmospheric mercury fluxes in northern Alaska: Global sources and Arctic depletion. *Environmental Science and Technology*, 39, 557–568. https://doi.org/10.1021/es049128x

Fu, X., Marusczak, N., Wang, X., Gheusi, F., & Sonke, J. E. (2016). Isotopic composition of gaseous elemental mercury in the free troposphere of the Pic du Midi Observatory, France. *Environmental Science and Technology*, 50 (11), 5641–5650. https://doi.org/10.1021/acs.est.6b00033

Fuller, C. C., van Geen, A., Baskaran, M., & Anima, R. (1999). Sediment chronology in San Francisco Bay, California, defined by 210Pb, 234Th, 137Cs, and 239,240 Pu. *Marine Chemistry*, *64*(1-2), 7-27. https://doi.org/10.1016/S0304-4203(98)00081-4

Ghosh, S., Schauble, E. A., Couloume, G. L., Blum, J. D., & Bergquist, B. A. (2013). Estimation of nuclear volume dependent fractionation of mercury isotopes in equilibrium liquid–vapor evaporation experiments. *Chemical Geology*, *336*, 5-12. https://doi.org/10.1016/j.chemgeo.2012.01.008

Goldberg, E. D. (1963). Geochronology with 210Pb radioactive dating. *International Atomic Energy Agency, Vienna, 121*, 130.

Gray, J. E., Pribil, M. J., Van Metre, P. C., Borrok, D. M., & Thapalia, A. (2013). Identification of contamination in a lake sediment core using Hg and Pb isotopic compositions, Lake Ballinger, Washington, USA. *Applied Geochemistry*, *29*, 1-12. https://doi.org/10.1016/j.apgeochem.2012.12.001

Guédron, S., Amouroux, D., Sabatier, P., Desplanque, C., Develle, A. L., Barre, J., Feng, C., Guiter, F., Arnaud, F., Reyss, J. L., & Charlet, L. (2016). A hundred year record of industrial and urban development in French Alps combining Hg accumulation rates and isotope composition in sediment archives from Lake Luitel. *Chemical Geology*, *431*, 10-19. https://doi.org/10.1016/j.chemgeo.2016.03.016

Huang, S., Sun, L., Zhou, T., Yuan, D., Du, B., & Sun, X. (2018). Natural stable isotopic compositions of mercury in aerosols and wet precipitations around a coal-fired power plant in Xiamen, southeast China. *Atmospheric Environment*, 173, 72-80. https://doi.org/10.1016/j.atmosenv.2017.11.003

Jiskra, M., Wiederhold, J. G., Skyllberg, U., Kronberg, R. M., Hajdas I., & Kretzschmar R. (2015). Mercury deposition and reemission pathways in boreal forest soils investigated with Hg isotope signatures. *Environmental Science and Technology*, *49*(12), 7188–7196. https://doi.org/10.1021/acs.est.5b00742

Jiskra, M., Wiederhold, J. G., Skyllberg, U., Kronberg, R. M., & Kretzschmar, R. (2017). Source tracing of natural organic matter bound mercury in boreal forest runoff with mercury stable isotopes. *Environmental Science: Processes and Impacts*, *19*(10), 1235-1248. DOI: 10.1039/C7EM00245A

Klump, J. V., Edgington, D. N., Sager, P. E., & Robertson, D. M. (1997). Sedimentary phosphorus cycling and a phosphorus mass balance for the Green Bay (Lake Michigan)

ecosystem. *Canadian Journal of Fisheries and Aquatic Sciences, 54*(1), 10-26. https://doi.org/10.1139/f96-247

Kurz, A. Y., Blum, J. D., Washburn, S. J., & Baskaran, M. (2019). Changes in the mercury isotopic composition of sediments from a remote alpine lake in Wyoming, USA. *Science of The Total Environment, 669*, 973-982. https://doi.org/10.1016/j.scitotenv.2019.03.165

Kwon, S. Y., Blum, J. D., Chirby, M. A., & Chesney, E. J. (2013). Application of mercury isotopes for tracing trophic transfer and internal distribution of mercury in marine fish feeding experiments. *Environmental Toxicology and Chemistry*, 32, 2322–2330. https://doi.org/10.1002/etc.2313

Kwon, S. Y., Blum, J. D., Yin, R., Tsui, M. T. K., Yang, Y. H., & Choi, J. W. (2020). Mercury stable isotopes for monitoring the effectiveness of the Minamata Convention on Mercury. *Earth-Science Reviews, 203*, 103111. https://doi.org/10.1016/j.earscirev.2020.103111

Lee, C. S., Lutcavage, M. E., Chandler, E., Madigan, D. J. Cerrato, R. M., & Fisher, N. S. (2016). Declining mercury concentrations in bluefin tuna reflect reduced emissions to the North Atlantic Ocean. *Environmental Science and Technology*, *50*(23), 12825-12830. https://doi.org/10.1021/acs.est.6b04328

Lepak, R. F., & Janssen, S. E. (2020a). Mercury Concentrations and Isotopic Compositions in Sediment Cores from North American Lakes (Alaska, Minnesota, and Newfoundland). U.S. Geological Survey Data Release. https://doi.org/10.5066/P9I5RL9C

Lepak, R. F., Janssen, S. E., Engstrom, D. R., Krabbenhoft, D. P., Tate, M. T., Yin, R., Fitzgerald, W. F., Nagorski, S. A., & Hurley, J. P. (2020b). Resolving Atmospheric Mercury Loading and Source Trends from Isotopic Records of Remote North American Lake Sediments. *Environmental Science and Technology*, *54*(15), 9325-9333. https://doi.org/10.1021/acs.est.0c00579

Li, C., Sonke, J. E., Le Roux, G., Piotrowska, N., Van der Putten, N., Roberts, S. J., Daley, T., Rice, E., Gehrels, R., Enrico, M., Mauquoy, D., Roland, T. P., & De Vleeschouwer, F. (2020). Unequal anthropogenic enrichment of mercury in Earth's northern and southern hemispheres. *ACS Earth and Space Chemistry*, *4*(11), 2073-2081. https://doi.org/10.1021/acsearthspacechem.0c00220

Lindberg, S., Bullock, R., Ebinghaus, R., Engstrom, D., Feng, X., Fitzgerald, W., Pirrone, N., Prestbo, E., & Seigneur, C. (2007). A synthesis of progress and uncertainties in attributing the sources of mercury in deposition. *Ambio*, 19-32. https://www.jstor.org/stable/4315781

Ma, J., Hintelmann, H., Kirk, J. L., & Muir, D. C. (2013). Mercury concentrations and mercury isotope composition in lake sediment cores from the vicinity of a metal smelting facility in Flin Flon, Manitoba. *Chemical Geology*, *336*, 96-102. https://doi.org/10.1016/j.chemgeo.2012.10.037

McKinney, M. A., Atwood, T. C., Pedro, S., & Peacock, E. (2017). Ecological change drives a decline in mercury concentrations in southern Beaufort Sea polar bears. *Environmental Science and Technology*, *51*(14), 7814-7822. https://doi.org/10.1021/acs.est.7b00812

Mergler, D., Anderson, H. A., Chan, L. H. M., Mahaffey, K. R., Murray, M., Sakamoto, M., & Stern, A. H. (2007). Methylmercury exposure and health effects in humans: a worldwide concern. *AMBIO: A Journal of the Human Environment*, *36*(1), 3-11. https://doi.org/10.1579/0044-7447(2007)36[3:MEAHEI]2.0.CO;2

Mulvaney, K.M., Selin, N.E., Giang, A., Muntean, M., Li, C.T., Zhang, D., Angot, H., Thackray, C.P., & Karplus, V.J. (2020). Mercury Benefits of Climate Policy in China: Addressing the Paris Agreement and the Minamata Convention Simultaneously. *Environmental Science and Technology*, *54*, 1326-1335. https://doi.org/10.1021/acs.est.9b06741

Percival, J. B., & Outridge, P. M. (2013). A test of the stability of Cd, Cu, Hg, Pb and Zn profiles over two decades in lake sediments near the Flin Flon Smelter, Manitoba, Canada. *Science of The Total Environment, 454*, 307-318. https://doi.org/10.1016/j.scitotenv.2013.03.011

Ren, L., Arkin, P., Smith, T. M., & Shen, S. S. (2013). Global precipitation trends in 1900–2005 from a reconstruction and coupled model simulations. *Journal of Geophysical Research: Atmospheres*, *118*(4), 1679-1689. https://doi.org/10.1002/jgrd.50212

Renedo, M., Amouroux, D., Duval, B., Carravieri, A., Tessier, E., Barre, J., Bérail, S., Pedrero, Z., Cherel, Y., & Bustamante, P. (2018). Seabird tissues as efficient biomonitoring tools for Hg isotopic investigations: Implications of using blood and feathers from chicks and adults. *Environmental Science and Technology*, *52*(7), 4227-4234. https://doi.org/10.1021/acs.est.8b00422

Renedo, M., Pedrero, Z., Amouroux, D., Cherel, Y., & Bustamante, P. (2021). Mercury isotopes of key tissues document mercury metabolic processes in seabirds. *Chemosphere*, *263*, 127777. https://doi.org/10.1016/j.chemosphere.2020.127777

Rydberg, J., Gälman, V., Renberg, I., Bindler, R., Lambertsson, L., & Martínez-Cortizas, A. (2008). Assessing the stability of mercury and methylmercury in a varved lake sediment deposit. *Environmental Science and Technology*, *42*(12), 4391-4396. https://doi.org/10.1021/es7031955

Selin, N. E. (2009). Global biogeochemical cycling of mercury: a review. *Annual Review of Environment and Resources*, *34*, 43-63. https://doi.org/10.1146/annurev.environ.051308.084314

Song, W., Li, A., Ford, J. C., Sturchio, N. C., Rockne, K. J., Buckley, D. R., & Mills, W. J. (2005). Polybrominated diphenyl ethers in the sediments of the Great Lakes. 2. Lakes Michigan and Huron. *Environmental Science and Technology*, *39*(10), 3474-3479. https://doi.org/10.1021/es048291p

Streets, D. G., Horowitz, H. M., Jacob, D. J., Lu, Z., Levin, L., Ter Schure, A. F., & Sunderland, E. M. (2017). Total mercury released to the environment by human activities. *Environmental Science and Technology*, *51*(11), 5969-5977. https://doi.org/10.1021/acs.est.7b00451

Sun, R., Sonke, J. E., Heimbürger, L. E., Belkin, H. E., Liu, G., Shome, D., Cukrowska, E. Liousse, C., Pokrovsky, O., & Streets, D. G. (2014). Mercury stable isotope signatures of world coal deposits and historical coal combustion emissions. *Environmental Science and Technology*, *48*(13), 7660-7668. https://doi.org/10.1021/es501208a

Sun, R., Streets, D. G., Horowitz, H. M., Amos, H. M., Liu, G., Perrot, V., Toutain, J-P., Hintelmann, H., Sunderland, E. M., & Mason, R. (2016). Historical (1850–2010) mercury stable isotope inventory from anthropogenic sources to the atmosphereMercury isotope emission inventory. *Elementa: Science of the Anthropocene*, 4. https://doi.org/10.12952/journal.elementa.000091

Sunderland, E. M. (2007). Mercury exposure from domestic and imported estuarine and marine fish in the US seafood market. *Environmental Health Perspectives*, *115*(2), 235-242. https://doi.org/10.1289/ehp.9377

United Nations Environment Programme. (2019). Minamata Convention on Mercury - Text and Annexes. Retrieved from http://www.mercuryconvention.org/Portals/11/documents/Booklets/COP3-version/Minamata-Convention-booklet-Sep2019-EN.pdf

Wasik, J. K. C., Engstrom, D. R., Mitchell, C. P. J., Swain, E. B., Monson, B. A., Balogh, S. J., Jeremiason, J. D., Branfireun, B. A., Kolka, R. K., & Almendinger, J. E. (2015). The effects of hydrologic fluctuation and sulfate regeneration on mercury cycling in an experimental peatland. *Journal of Geophysical Research: Biogeosciences*, 120(9), 1697-1715. https://doi.org/10.1002/2015JG002993

Wiederhold, J. G., Cramer, C. J., Daniel, K., Infante, I., Bourdon, B., & Kretzschmar, R. (2010). Equilibrium mercury isotope fractionation between dissolved Hg (II) species and thiol-bound Hg. *Environmental Science and Technology*, *44*(11), 4191-4197. https://doi.org/10.1021/es100205t

Yin, R., Feng, X., Hurley, J. P., Krabbenhoft, D. P., Lepak, R. F., Kang, S., Yang, H., & Li, X. (2016a). Historical records of mercury stable isotopes in sediments of Tibetan lakes. *Scientific Reports*, *6*, 23332. https://doi.org/10.1038/srep23332

Yin, R., Lepak, R. F., Krabbenhoft, D. P., & Hurley, J. P. (2016b). Sedimentary records of mercury stable isotopes in Lake Michigan. *Elementa: Science of the Anthropocene*, *4*. https://doi.org/10.12952/journal.elementa.000086

Zdanowicz, C. M., Krümmel, E. M., Poulain, A. J., Yumvihoze, E., Chen, J., Štrok, M., Scheer, M. & Hintelmann, H. (2016). Historical variations of mercury stable isotope ratios in Arctic

glacier firn and ice cores. *Global Biogeochemical Cycles*, *30*(9), 1324-1347. https://doi.org/10.1002/2016GB005411

Zerkle, A. L., Yin, R., Chen, C., Li, X., Izon, G. J., & Grasby, S. E. (2020). Anomalous fractionation of mercury isotopes in the Late Archean atmosphere. *Nature Communications*, *11*(1), 1-9. https://doi.org/10.1038/s41467-020-15495-3

Zhou, J., Obrist, D., Dastoor, A., Jiskra, M., & Ryjkov, A. (2021). Vegetation uptake of mercury and impacts on global cycling. *Nature Reviews Earth & Environment*, 1-16. https://doi.org/10.1038/s43017-021-00146-y